Hindawi Publishing Corporation
EURASIP Journal on Advances in Signal Processing
Volume 2008, Article ID 453218, 11 pages
doi:10.1155/2008/453218

Research Article

A Simple Technique for Fast Digital Background Calibration of A/D Converters

Francesco Centurelli, Pietro Monsurrò, and Alessandro Trifiletti

Dipartimento di Ingegneria Elettronica, Università di Roma La Sapienza, Via Eudossiana 18, 00184 Roma, Italy

Correspondence should be addressed to Francesco Centurelli, centurelli@mail.die.uniroma1.it

Received 30 April 2007; Revised 4 August 2007; Accepted 28 October 2007

Recommended by C. Vogel

A modification of the background digital calibration procedure for A/D converters by Li and Moon is proposed, based on a method to improve the speed of convergence and the accuracy of the calibration. The procedure exploits a colored random sequence in the calibration algorithm, and can be applied both for narrowband input signals and for baseband signals, with a slight penalty on the analog bandwidth of the converter. By improving the signal-to-calibration-noise ratio of the statistical estimation of the error parameters, our proposed technique can be employed either to improve linearity or to make the calibration procedure faster. A practical method to generate the random sequence with minimum overhead with respect to a simple PRBS is also presented. Simulations have been performed on a 14-bit pipeline A/D converter in which the first 4 stages have been calibrated, showing a 15 dB improvement in THD and SFDR for the same calibration time with respect to the original technique.

1. INTRODUCTION

Wireless communication has become one of the main drivers for high-resolution, high-speed analog-to-digital converters (ADCs). There is a strong trend in communication systems to push the border of digital conversion toward the transmit and receive terminals, and to implement as much functionality as possible in the digital domain to reduce the cost and increase the reliability and flexibility of the system. This stresses the requirements on analog-to-digital converters both in terms of precision and conversion speeds: in some applications, 12–14 bits at hundreds of MHz conversion rate could be required [1], in addition to restrictions on maximum power consumption to allow the use in portable applications.

These requirements impose the use of pipelined ADCs; however, in practical switched-capacitor implementations, the ADC performance is limited by circuit nonidealities such as finite opamp gain and bandwidth, and process-related mismatch in capacitors. Some form of calibration is thus required to compensate for these effects, and this also allows relaxing the specifications on the stages of the pipeline, resulting in lower power dissipation and area consumption. The availability of large digital signal processing capability on-chip at very low power and area cost allows the complexity of calibration to move from the analog to the digital domain.

Many digital self-calibration schemes working in foreground have been presented in the literature [2, 3], but they require the ADC to be offline. To solve this problem, interpolation (e.g., skip and fill) algorithms [4] or slot queues [5] have been proposed, or some redundancy can be introduced in the system to allow offline calibration of single stages [6]. A more elegant solution has been proposed by digital background calibration algorithms that are able to work without interfering with the normal ADC operation [7–9]. In these techniques, the analog error is modulated by a pseudorandom sequence, and then the digital output is processed in order to extract the modulated information needed to correct the ADC performance.

In these digital background calibration techniques based on statistical error estimation, fast convergence represent an important requirement. If error parameters are not constant in time, for example, the calibration procedure will continuously track these variations in order to optimize the system linearity. Unfortunately, there is a tradeoff between convergence speed and calibration accuracy, due to the statistical

nature of the background calibration procedure. This procedure estimates the (small) error parameters by filtering a signal that contains also several unwanted wideband terms, the largest of which is due to the input signal. A very narrowband filter is thus needed to improve the SNR of the estimation, resulting in a convergence which slows down as the desired accuracy gets higher. In [9, 10] this problem is addressed by splitting the ADC into two nominally identical channels and estimating the error terms considering the difference between the two channels output, thus ideally removing the input signal; in [11], on the other hand, the input signal is interpolated by use of Lagrange interpolation and the predicted input signal level is used to reduce its impact on the process of estimation of the error terms.

The availability of high-resolution, high-speed ADCs allows IF filtering and demodulation to be performed in the digital domain, so that RF receivers for different standards can be implemented on a single hardware platform. In this situation, the input to the ADC is a narrowband signal, with no information content at dc, and occupies only a fraction of the Nyquist bandwidth. This knowledge can be exploited in the digital background calibration procedure to get a faster convergence or a lower error on the estimate of the correction word. In this paper, we present a modification to the calibration procedure in [9] to be used with narrowband signals. The same technique with just slight modifications can also be exploited with baseband signals, with a penalty on the maximum allowable input signal bandwidth. What is needed is a section of the spectrum without information content, as can be obtained, for example, at the end of the Nyquist band through the use of an antialiasing filter with a bandwidth slightly lower than the Nyquist frequency.

This paper is organized as follows. In Section 2, the standard calibration procedure is briefly described. In Section 3, the modified method optimized for narrowband signals is presented, and issues related to its implementation are discussed. Section 4 presents some simulations to verify the advantages of the proposed method, and Section 5 compares our technique with other proposed techniques which address the same problem.

2. STANDARD DIGITAL BACKGROUND CALIBRATION

A pipeline ADC is composed of a cascade of stages that perform an analog-to-digital conversion with a limited number of bits and calculate the conversion residue to be converted by the following stages, as shown in Figure 1. The stages are typically implemented using switched-capacitor circuits, and the sub-DAC, the subtraction block, the amplification, and the sample-and-hold functions are merged in a single circuit called multiplying digital-to-analog converter (MDAC). Redundant signed digit (RSD), also known as digital error correction (DEC), is used to tolerate errors in the sub-ADC [12]. A commonly used architecture is the 1.5-bit-per-stage ADC, where each stage produces 2 bits with one bit of redundancy, but only three configurations of bits are allowed.

The precision of the conversion is affected by errors in the interstage gain R (called radix), due to capacitor mismatch, finite opamp gain, and incomplete settling. Digi-

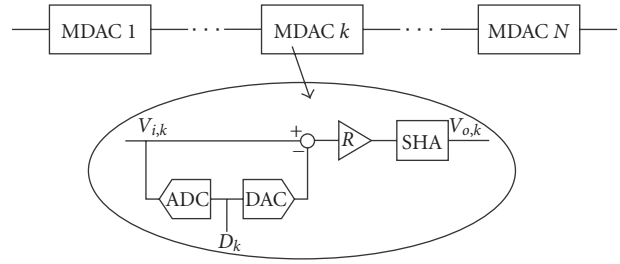

Figure 1: Block scheme of a pipeline ADC.

tal background calibration algorithms based on correlation techniques estimate the effective interstage gain R and calculate the correct ADC output by digital signal processing, while the ADC is in operation and without requiring additional analog hardware. These techniques introduce a random signal, uncorrelated with the input signal, at some point into the MDAC: this is just an additive noise for the pipeline, but the correlation of the ADC output with the same random signal allows estimating the effective radix.

The output residue of the kth ideal pipeline stage can be written as

$$V_{o,k} = 2V_{i,k} - D_k V_R, \tag{1}$$

where $V_{i,k}$ is the stage input signal, V_R is the reference voltage, D_k is the digital output (-1, 0, or 1), and the radix is 2. The input-output relationship for an ideal ADC is therefore

$$V_i = \sum_{k=1}^{N} \frac{D_k}{2^k} V_R + Q_N = \hat{V}_i + Q_N, \tag{2}$$

where V_i is the overall input signal, Q_N is the quantization error (residue of the Nth stage), and $\hat{V}_i$ is the reconstructed input signal. When errors due to capacitor mismatch and finite opamp gain are taken into account, (1) can be rewritten as

$$V_{o,k} = R_k \left(V_{i,k} - \frac{D_k V_R}{2} \right), \tag{3}$$

where R_k is the effective radix.

The true ADC input-output relationship is therefore

$$V_i = \sum_{k=1}^{N} \frac{D_k}{\prod_{j=1}^{k-1} R_j} \frac{V_R}{2} + Q_N, \tag{4}$$

and the correct digital output could be calculated as

$$D_o = \sum_{k=1}^{N} D_k \prod_{j=k}^{N-1} R_j \tag{5}$$

if the radices were known. By using the ideal values $R_j = 2$ (i.e., by interpreting the digital output D_o as a binary number) an error occurs; a calibration procedure is therefore needed to calculate the corrected digital output D_{oC} such that

$$\hat{V}_i = \frac{V_R D_{oC}}{2^N} = V_i - Q_N. \tag{6}$$

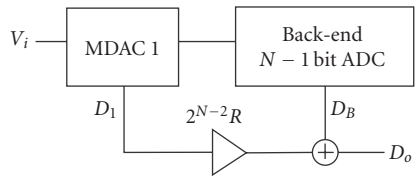

Figure 2: Block scheme for the calibration of the first MDAC.

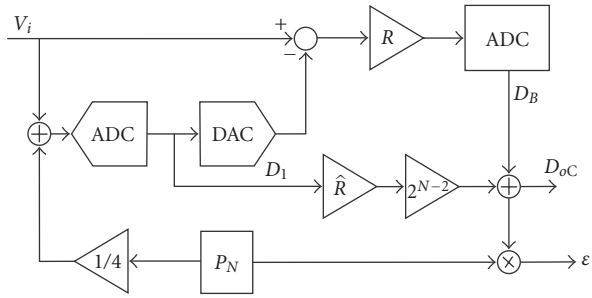

Figure 3: Block scheme of the calibration technique by correlation.

An estimation of the true radices R_j is needed to calculate D_{oC}.

Precision requirements on the stages reduce as we proceed along the pipeline; only the first stages of the pipeline therefore will need calibration, and the estimations of the effective radices of the stages will converge from the end of the pipeline towards the first MDAC. We consider the calibration algorithm proposed by Li and Moon in [9], and in the following we describe the calibration process for a single stage: the pipeline ADC can be decomposed in a first stage to be calibrated, that provides the digital output D_1, and a backend ideal $(N-1)$-bit ADC that provides the output D_B, as shown in Figure 2. The correct ADC digital output would be therefore

$$D_o = 2^{N-2}RD_1 + D_B. \tag{7}$$

To estimate the radix R of the MDAC, a random sequence P_N can be added at the input of the flash ADC as shown in Figure 3. This sequence has to be uncorrelated with the input signal, and usually a pseudo-white noise is used, as can be provided by a PRBS generator of adequate length. The true digital output can still be calculated by (7) using the radix estimate $\hat{R}$, and the conversion error reduces to the quantization noise Q_N as the estimate converges:

$$V_i - \hat{V}_i = \frac{R}{\hat{R}}Q_N - \left(\frac{P_N}{4} - Q_1\right)\left(1 - \frac{R}{\hat{R}}\right), \tag{8}$$

where Q_1 is quantization error of the first stage,

$$\hat{V}_i = \frac{V_R D_{oC}}{2^{N-1}\hat{R}} \tag{9}$$

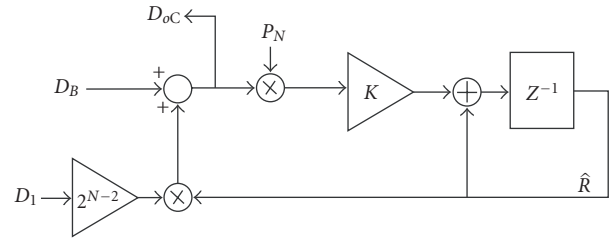

Figure 4: Practical implementation of the estimation technique by correlation.

is the reconstructed input signal, and

$$D_{oC} = 2^{N-2}\hat{R}D_1 + D_B \tag{10}$$

is the corrected digital output. By correlating the digital output (10) with the PRBS sequence, we can calculate the estimation error and update the radix estimate to use in (10):

$$(P_N \otimes D_{oC})\frac{V_R}{2^{N-1}} = P_N \otimes \hat{R}V_i - P_N \otimes RQ_N + P_N \otimes (R-\hat{R})Q_1 - P_N \otimes \frac{P_N}{4}(R-\hat{R}), \tag{11}$$

(where $\otimes$ means correlation and a scaling factor has been used) that converges to

$$\varepsilon = -\frac{(R-\hat{R})}{4} \tag{12}$$

since $P_N \otimes P_N = 1$ and $P_N \otimes V_i = 0$, $P_N \otimes Q_1 \cong 0$, $P_N \otimes Q_N \cong 0$.

A practical way to calculate (12) and update the corrected digital output (10) is shown in Figure 4: a zero-forcing loop is constructed to drive to zero the average value of $P_N D_{oC}$. This occurs when the correct estimate of the radix R is used, as shown in (11), thus the correct digital output D_{oC} is obtained, and that is a linearized version of D_o. K is a gain factor which sets the bandwidth of the filter, determining the tradeoff between speed and accuracy.

3. DIGITAL BACKGROUND CALIBRATION WITH COLORED RANDOM SEQUENCE

3.1. Modified calibration procedure for narrowband signals

In the calibration technique presented in the previous section, the correlation (11) is calculated in practice by multiplying the output signal D_{oC} by the random sequence P_N, and lowpass filtering the result. This provides an error term θ_{err} in addition to (12) which is due to the energy of the undesired terms in (11) (all except the last) inside the filter bandwidth: since the quantization error is much smaller than the input signal, we have

$$\theta_{\text{err}} \cong P_N \otimes \hat{R}V_i. \tag{13}$$

This is the main contribution to the signal-to-calibration-noise-ratio (SCNR), which is an error introduced on

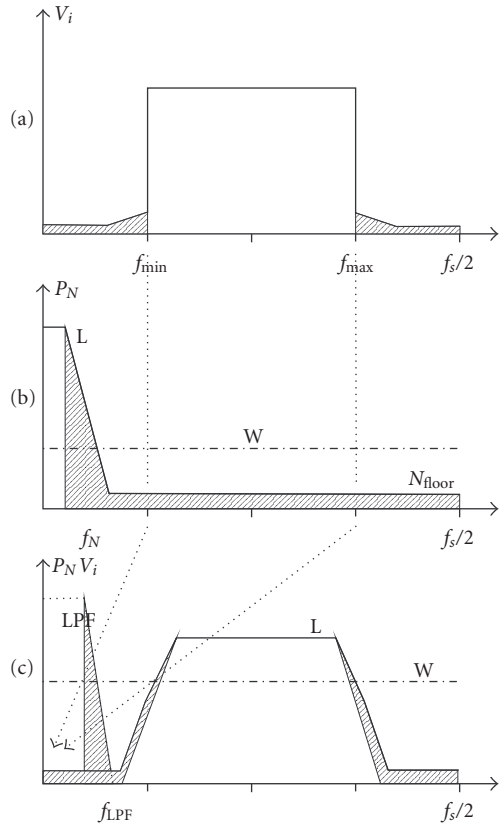

Figure 5: Power density spectra of the input signal (a), the random sequence (b), and their product (c) in case of ideal and nonideal (shaded area) lowpass filters.

the estimation process because filtering cannot be perfect in order to be possible in a finite time. It has to be noted that the term in Q_1 is small since it is proportional to the estimation error. The technique we are going to propose reduces the power of the error term (13), thus allows a better and faster estimation of the true radix.

If P_N is white, the term $P_N\hat{R}V_i$ will also be white; thus the total noise at the output of the filter will depend on the bandwidth of the filter itself. A tradeoff has to be found between estimation noise minimization, that requires a very narrow bandwidth, and convergence time, that is inversely proportional to the bandwidth [11]; a higher-order filter does not help to solve the tradeoff since for a white input noise the total output power is roughly proportional to the bandwidth of the filter

This tradeoff can be overcome if the input signal to be converted does not occupy the full Nyquist bandwidth: this case is quite common in analog-to-digital converters for wireless applications, where the received IF signal is digitized and then downconverted to baseband in the digital domain, so that there is no information content at the two extremes of the Nyquist band. It is therefore possible to spectrally separate the random sequence P_N and the signal V_i, thus allowing a reduction of the low-frequency noise at the input of the filter, which will now be able to estimate the error term ε more easily.

Let us suppose that the random sequence P_N is obtained by lowpass filtering a PRBS, and that its spectrum and the spectrum of the input signal V_i do not overlap (let $f_{\min}$ be the minimum frequency of the signal). Their product therefore does not contain any dc component, and an ideal lowpass filter can perfectly eliminate the estimation noise θ_{err} and provide the estimation error (12). Moreover, the calibration residue on the digital output, due to the use of an incorrect estimate of the radix in (10), appears as a noise component outside the bandwidth of the signal, and can be eliminated by the subsequent digital processing. Figure 5 shows the power density spectrum (psd) of the term $P_N\hat{R}V_i$ in case of a white random signal (labeled W) and of a PRBS filtered by an ideal lowpass filter with bandwidth f_N (labeled L; neglect the shaded area). In the latter case, there is no component in the lower end of the spectrum, so that the estimate (12) can be obtained with an ideal lowpass filter with bandwidth f_{LPF} as large as $f_{\min} - f_N$, with a net increase both in SNR (which ideally goes to infinity) and in convergence time.

Even if nonideal lowpass filters are considered, both for the generation of P_N and for filtering the product $P_N D_{oC}$, it can be shown that the use of a colored random sequence P_N allows more flexibility in finding the optimal tradeoff between SNR of the estimate and convergence time. To analyze this case, let us remove the simplifying assumptions from the situation discussed before, considering the shaded areas in Figure 5. The spectrum of the input signal V_i presents tails below $f_{\min}$; however, if a high-precision ADC is considered, we can assume that the noise has been minimized, thus in the following we will continue supposing the input signal bandlimited. The random sequence P_N is obtained by lowpass filtering a white noise, so its power density will decrease with a finite slope after the filter bandwidth f_N; a noise floor N_{floor} will also be present due to quantization effects. The maximum allowable bandwidth for the lowpass filter is reduced with respect to the ideal case, due to the slope of the spectrum of P_N. Moreover, the noise floor of the random sequence produces a component inside the bandwidth f_{LPF} of the lowpass filter, that results in estimation noise.

The noise term θ_{err} is given by the energy of the product $P_N V_i$ inside the bandwidth of the lowpass filter f_{LPF}; we can estimate its value by neglecting the sidelobes of the signal. We get $\theta_{\text{err}} \propto \sqrt{N_{\text{floor}} f_{\text{LPF}} B}$ where B is the signal bandwidth; this can be compared with the result we get for a white random sequence P_N with power spectral density N_W, that is, $\theta_{\text{err}} \propto \sqrt{N_W f_{\text{LPF}} B}$. The proposed technique reduces the noise floor for the frequencies inside the bandwidth of the signal, thus allowing an improvement in the SCNR of the estimation given by the ratio between the power density of the white noise N_W and the noise floor of the colored sequence N_{floor}:

$$\Delta\text{SCNR} = \frac{N_W}{N_{\text{floor}}}. \tag{14}$$

This assumes that the filter bandwidth f_{LPF} and its order have been chosen to reach the noise floor well before the minimum frequency of the signal.

The spectrum in Figure 5(c) allows to make some considerations on the lowpass filter to be used to extract the estimation error (12): since the spectrum of $P_N D_{oC}$ is not white, the filter should avoid to include the central part of the spectrum to minimize the error θ_{err}. If such condition is respected, the same tradeoff between precision and velocity of the estimation as for the white noise case applies; the improvement in the SCNR however allows a much higher precision for the same bandwidth of the filter, or a wider bandwidth can be used to achieve faster convergence with the same (or even lower) error than for the white P_N case with a ratio given by (14). In this case, a higher-order filter can be used to increase the bandwidth f_{LPF} (and so reduce convergence time) filtering out the excess noise due to the central part of the spectrum of $P_N D_{oC}$.

3.2. Calibration of baseband signals

A colored random sequence can be used to get faster convergence or more accurate estimation even if the input signal V_i is not narrowband and presents a dc component: in this case, the spectrum of the random sequence has to be concentrated at the high end of the Nyquist bandwidth, and a penalty has to be paid in terms of the maximum allowable frequency of the input signal, that has to be lower than $f_s/2$ of at least the bandwidth of the filter to be used for estimation and the bandwidth of the PRBS signal:

$$f_{\max} < \frac{f_s}{2} - (f_{\text{LPF}} + f_N). \tag{15}$$

In this case, the P_N sequence should have a highpass spectrum, in order to occupy a different band with respect to the input signal. This highpass sequence can be obtained by a lowpass sequence by modulating it with the sequence $(-1)^k$. The Nyquist band around $f_S/2$ may be free from signal content because of the antialiasing filter. Because ideal antialiasing filters do not exist, our technique may use a part of the spectrum which for some other reason (e.g., finite slope of the filter) is not employed, with no real loss in bandwidth.

3.3. Calibration of multiple stages

If we consider the calibration of two stages, we need to have two colored uncorrelated noise sequences, P_{N1} and P_{N2}, and add them at the two stages to be calibrated. If we assume for simplicity that each stage can be described by the relation (3), we can write for the output of the second stage:

$$\begin{aligned} V_{o,2} &= R_1 R_2 V_i - R_1 R_2 D_1 \frac{V_R}{2} - R_2 D_2 \frac{V_R}{2} \\ &= \frac{D_B V_R}{2^{N-2}} + R_1 R_2 Q_N, \end{aligned} \tag{16}$$

where R_1 and R_2 are the radices of the two stages, D_1 and D_2 are their digital outputs, D_B is the digital output of the back-end $(N-2)$-bit ADC, and Q_N is the overall quantization error. The overall digital output, when the estimated radices $\hat{R}_1$ and $\hat{R}_2$ are used, is given by

$$D_{oC} = 2^{N-3} \hat{R}_2 \hat{R}_2 D_1 + 2^{N-3} \hat{R}_2 D_2 + D_B, \tag{17}$$

and by correlating it by the pseudorandom sequence of the second stage P_{N2} we get

$$\begin{aligned} &(P_{N2} \otimes D_o) \frac{V_R}{2^{N-2}} \\ &\quad = P_{N2} \otimes \hat{R}_1 \hat{R}_2 (V_i - Q_N) + P_{N2} \otimes \frac{\hat{R}_1}{R_1} Q_2 (R_2 - \hat{R}_2) \\ &\qquad - P_{N2} \otimes \frac{P_{N2}}{4} \frac{\hat{R}_1}{R_1} (R_2 - \hat{R}_2), \end{aligned} \tag{18}$$

that is similar to (11). The last term in (18) has a mean value proportional to the estimation error $R_2 - \hat{R}_2$. The other terms have a zero mean value and constitute the estimation noise: the only significant term is the first, and for it the same considerations as in the previous subsection apply. The term in Q_2 (quantization error of the second stage) cannot be considered narrowband, but its impact is limited since it is proportional to the estimation error.

3.4. A practical method to generate P_N

The sequence P_N we are proposing to use for the correlation technique is a colored noise with its spectrum concentrated at low frequencies, and can be obtained by lowpass filtering a PRBS signal (pseudo-white noise) and quantizing the filter output at one bit. This implementation is however quite power and area hungry, since the filter needs a large number of bits to avoid finite word-length effects. We propose here a more efficient way to generate the desired random sequence, by nonlinear processing of a PRBS signal.

We can observe that a random signal with its spectrum concentrated at low frequencies presents a high level of correlation between subsequent bits, and therefore a low probability of transition, whereas the probability of transition for a PRBS sequence is 0.5. However, for a PRBS $2^N - 1$, the probability to have L (<N) consecutive identical bits is 2^{-L}: we can therefore generate a colored random sequence by forcing a transition every time the PRBS presents L consecutive identical bits, where L is chosen to obtain the desired spectral behavior. Figure 6 shows a possible implementation, where the shift register and the L-input AND generate a sequence T, that is used to generate a Markovian stochastic process P_N defined by the following relation:

$$P_N[k] = \begin{cases} P_N[k-1] & \text{if } T[k] = 0, \\ \overline{P_N}[k-1] & \text{if } T[k] = 1. \end{cases} \tag{19}$$

For the sequence P_N, the probability to have a 0 or a 1 is equal by symmetry; however, the probability to have two consecutive identical bits is $1–2^{-L}$ and the probability to have a transition is 2^{-L} by construction.

The same scheme can be used to generate a random sequence with its spectrum concentrated around $f_s/2$, by substituting the AND gate with NAND, so to have a very high probability of transition $(1–2^{-L})$.

The sequence has most of its power concentrated around dc or $f_S/2$, and since the total power remains constant the

Table 1: Noise bandwidth versus L.

L	BW 50%	BW 90%
1 (white)	50%	90%
3	4.5%	56%
5	0.8%	6%
7	0.2%	1.2%
9	0.05%	0.3%
11	0.02%	0.15%

noise floor becomes lower than the white noise level. This enables the SCNR improvement described previously. Table 1 shows the bandwidth of the PRBS as a function of L. For each value of L, we report the fraction of the Nyquist bandwidth in which 50% and 90% of the noise power is concentrated. The former is a good approximation of the 3 dB bandwidth of the noise f_N if a first-order LPF is assumed, and simulations show a 20 dB/decade slope in the noise spectrum.

Figure 7 shows the psd of the colored noise sequence in case of $L = 9$ and spectrum concentrated at $f_s/2$; the psd of a white noise of the same power is shown for comparison (frequency is normalized to the Nyquist frequency $f_S/2$).

If the first M stages of the pipeline have to be calibrated using the proposed method, M uncorrelated noise sequences are needed. These sequences can be generated by using the L-input AND scheme in Figure 6 starting from M uncorrelated white sequences. A single PRBS generator can be used, since two shifted copies of the same white sequence are uncorrelated. However, large shifts are needed if we want also the outputs of the AND gates to be uncorrelated: a simple solution is proposed in [13], where a large shift between copies of a PRBS sequence is obtained by performing the exclusive OR operation between copies with small shifts.

4. SIMULATIONS

In this section, we present some simulations of the proposed technique in MATLAB environment, to assess its advantages over the standard technique when narrowband input signals are considered. The technique has been applied to a pipeline ADC with 14-bit nominal resolution, to calibrate the first stage where an error on the radix R has been forced. Monte Carlo iterations have been performed for the parameter R varying in a suitable range (a Gaussian distribution with a 0.2% standard deviation has been assumed).

We have considered an input signal composed of 8 tones around the center of the Nyquist bandwidth. The random sequence is generated from a PRBS $2^{32} - 1$, according to the method described in the previous section, choosing $L = 10$ (this corresponds to a bandwidth f_N of about 0.035% of the Nyquist bandwidth); for comparison, the same PRBS has been used as the random signal P_N in a standard implementation of the calibration procedure.

The use of a colored noise sequence allows to have a much lower estimation error for the same bandwidth of the filter, as is shown in Figure 8, that reports the transient response of the estimation, respectively, for the standard implementation and for the proposed implementation (the initial estimate of the radix is zero, and 100 Monte Carlo iterations are reported). In this case, the same filter bandwidth (21 ppm of the Nyquist bandwidth) enables a large reduction in SCNR for the same calibration speed.

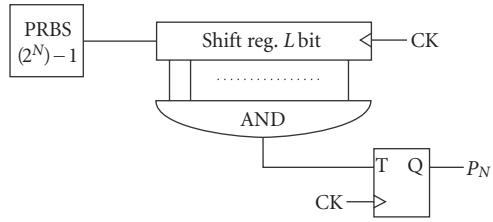

Figure 6: Generation of a colored random sequence.

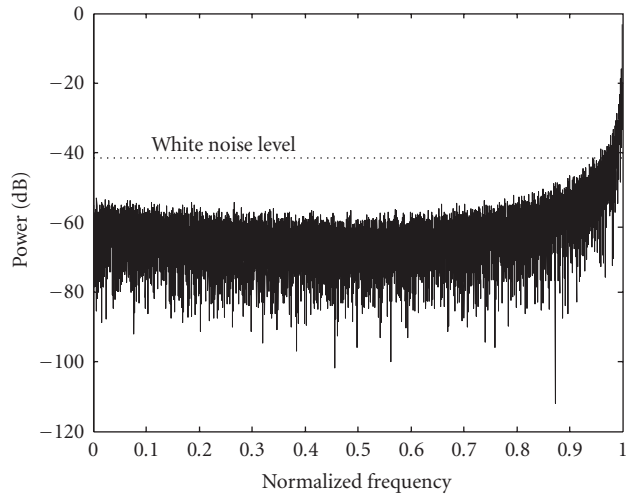

Figure 7: Power density spectrum of the colored noise for $L = 9$.

Figure 9 shows the transient response when a 100-times larger lowpass filter is used for the proposed implementation: this allows a faster convergence of the estimation, with a lower residue error than for the standard implementation (note the different scale on x-axis). Despite the 100-times faster filter, SCNR still seems lower than in the standard case.

The lower estimation error of the proposed calibration technique allows a better calibration with lower noise. To verify this, we have simulated a pipeline ADC with 14 nominal bits of resolution, composed of 13 identical 1.5-bit stages. Each stage has gain errors with a variance of 1%, offset errors (for the MDAC and the comparators) of 1%, and third-order nonlinearity at the output of the MDAC stage with a variance of 0.1%. This results in variance of the radix of about 1.75%, and some nonlinear error. The input signal is composed of four nonmodulated carriers around $f_s/4$; they have the same amplitude, which is a quarter of the full scale range of the ADC. The gain K used for calibration has been set to 2^{-18}, and the colored random sequences have been obtained using $L = 9$. Calibration has been applied to the first four stages.

Figure 10 shows the spectrum of the output signal without calibration and when calibrated with the standard and proposed simulation technique. The same filter with bandwidth of 5.4 ppm of the Nyquist frequency is used, and the

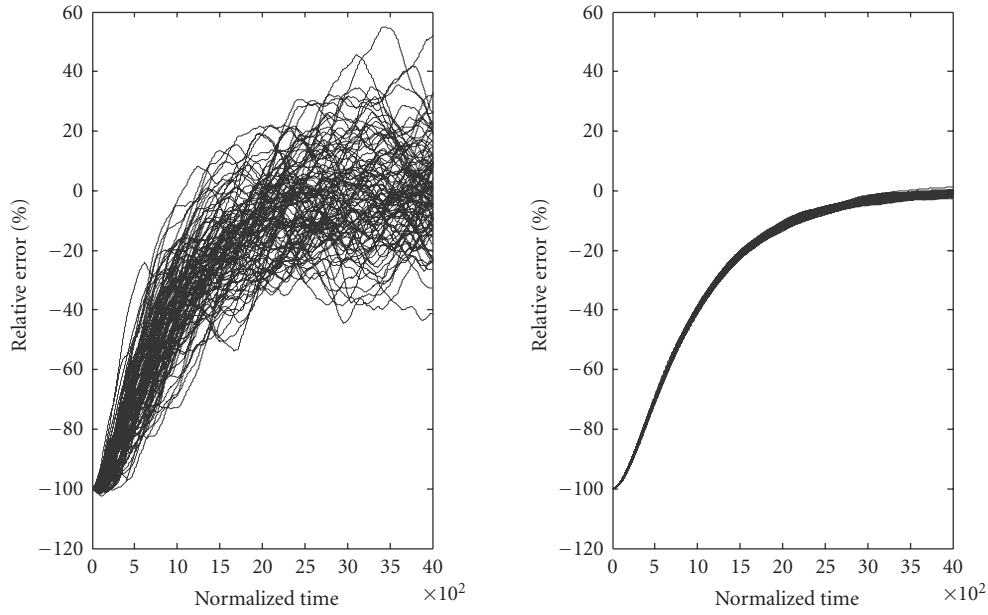

Figure 8: Transient response of the standard (a) and proposed (b) method, for the same bandwidth of the estimation filter (100 Monte Carlo iterations).

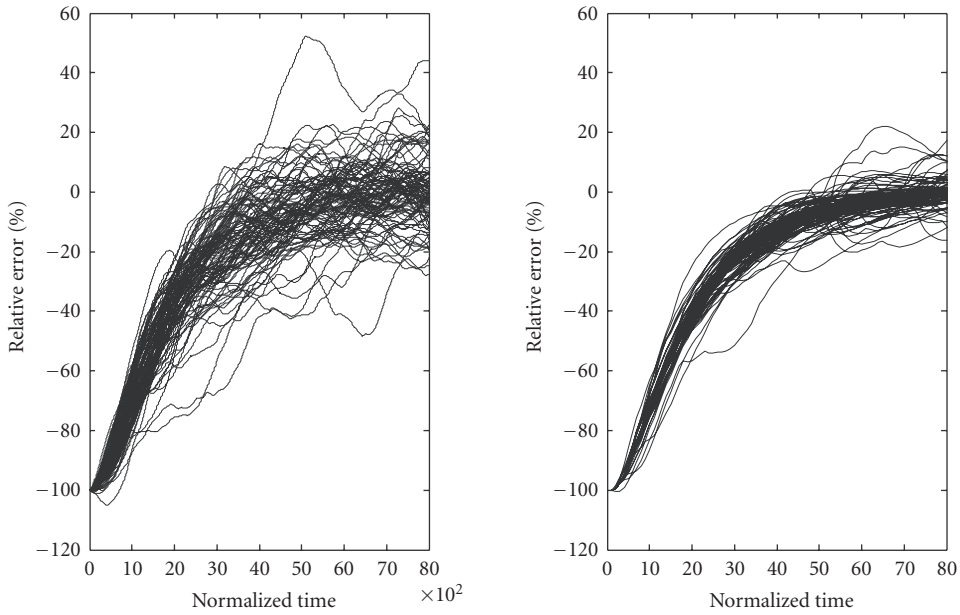

Figure 9: Transient response of the standard (a) and proposed (b) method, when a 100-times larger lowpass filter is used (100 Monte Carlo iterations).

colored sequence presents a noise floor of about 20 dB lower than the white noise level.

Figure 11 shows the histograms of the effective number of bits (ENOB) with and without calibration, for 100 Monte Carlo iterations, and Table 2 reports the average value and standard deviation of ENOB and SFDR.

Figure 12 shows the transient evolution of the ENOB as the ADC gets calibrated: the same filter bandwidth is used in both cases, providing the same convergence time, with a different estimation noise, thus a different ADC precision. In the standard calibration case, the chosen bandwidth results in an excessive calibration noise, due to the undesidered

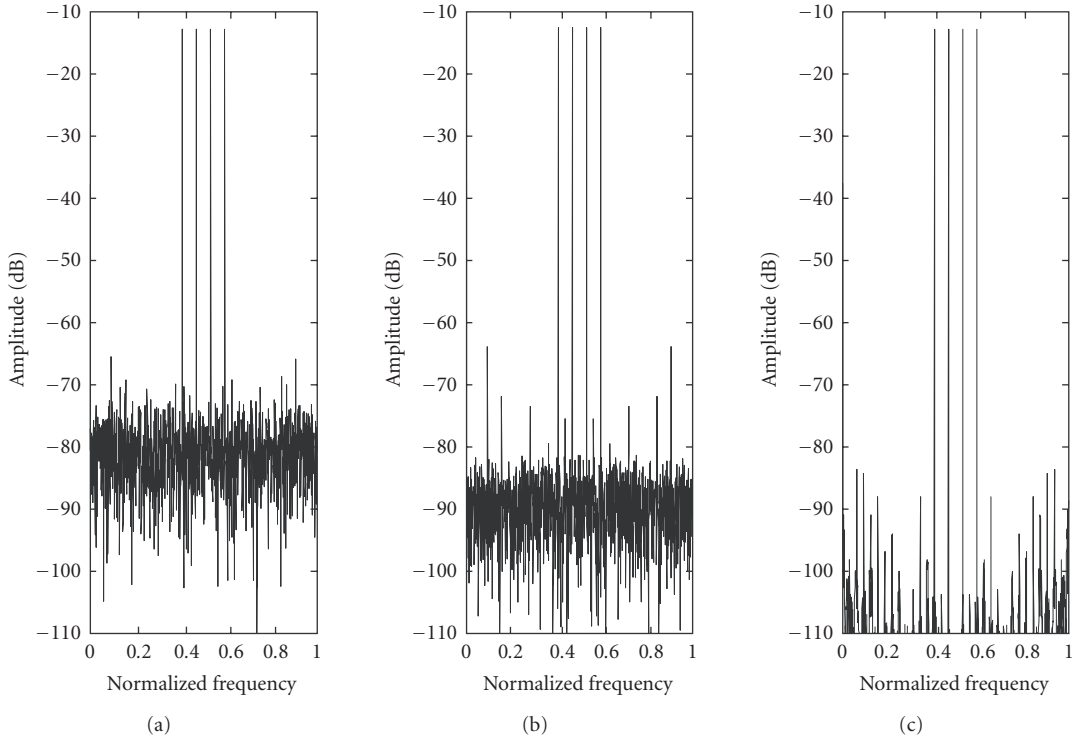

Figure 10: Output spectrum of the ADC: (a) output signal without calibration; (b) with standard calibration; (c) with the proposed calibration.

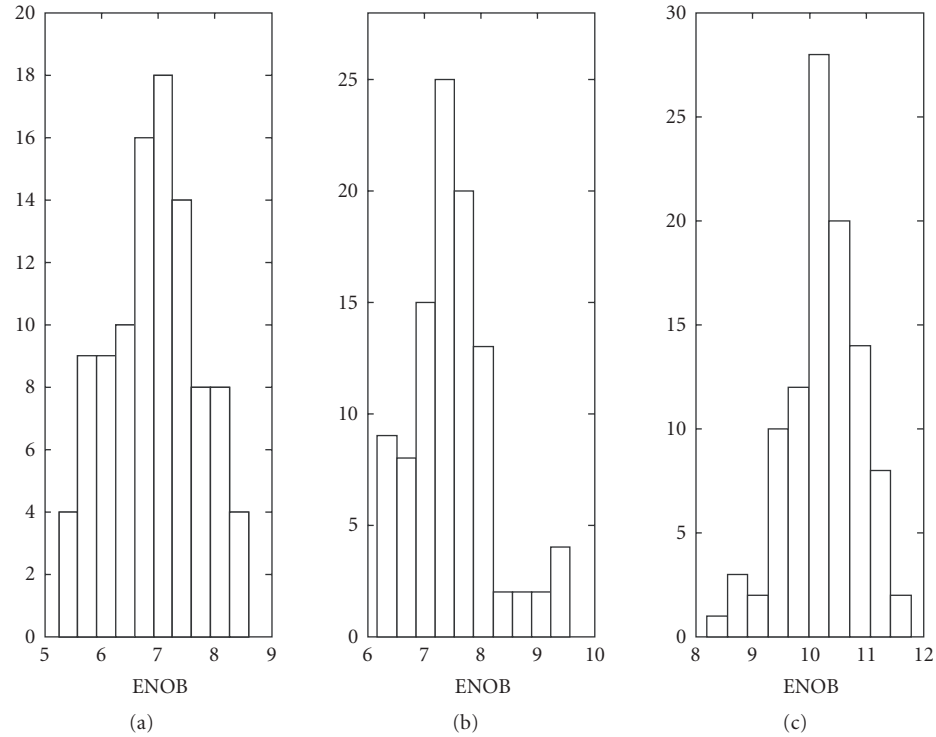

Figure 11: ENOB histograms: (a) without calibration; (b) standard calibration; (c) proposed calibration.

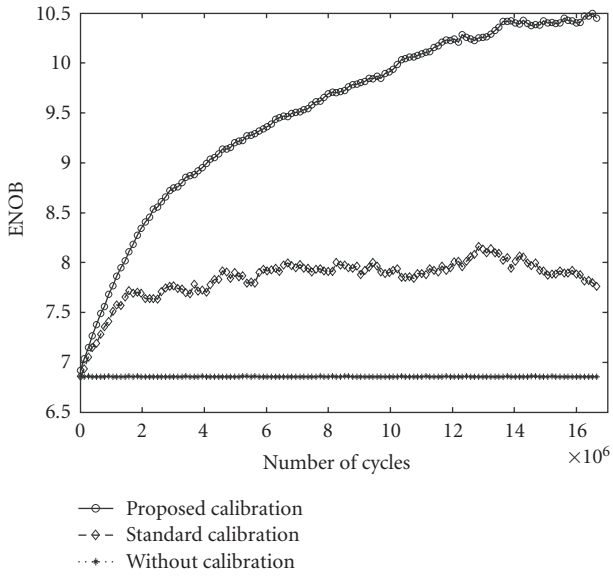

Figure 12: Transient evolution of the ENOB during calibration (same filter for standard and proposed calibration).

Table 2: Precision performance of the ADC.

	No. calibration	Standard calibration	Proposed calibration
ENOB: mean	6.9 bits	7.8 bits	10.5 bits
ENOB: std	0.8 bits	0.6 bits	0.6 bits
SFDR: mean	48 dB	54 dB	68 dB
SFDR: std	5.4 dB	4.3 dB	4.2 dB

terms in (11) and in particular to the input signal. If the estimation noise is comparable with the error term to be estimated, calibration does not improve linearity, and the ENOB presents wide oscillations around its average value.

Figure 13 shows the spectrum of $V_{IN}P_N$ in case of a white PRBS and a colored noise sequence: a 20 dB improvement in the power at low frequencies, which results in the error term (13), is evident.

If a smaller filter bandwidth is used in the standard calibration case, we get a slower convergence with a smaller error. Figure 14 shows the transient evolution of the ENOB when the gain K is 2^{-16} for the proposed method and 2^{-20} for the standard calibration, that results in a factor 16 on the filter bandwidth.

5. COMPARISON WITH EXISTING TECHNIQUES

Different techniques have been presented in the literature to improve the convergence speed of the calibration procedure by cancellation of the interference due to the input signal. In [9, 10] the input signal is cancelled by using two identical half-sized pipeline A/D converters in parallel, fed by the same signal, and by extracting the error terms by filtering off the difference between the two channels' outputs. If the two channels are identical, cancellation of the input interference term is perfect, and calibration can be done much faster; however, if the two channels are mismatched, cancellation is incomplete and the interference term is attenuated but not cancelled. Sensitivity to channel mismatches limits in practice the appeal of this technique: whereas the ADCs could be scaled to exploit the calibration to achieve good accuracy with low area and power consumption, this increases the mismatch between the channels reducing the effectiveness of the calibration technique. Moreover, half-sizing the two channels would worsen the mismatch, so that larger stages would have to be used, with an increase in area and power consumption with respect to a simple ADC. This issue has been addressed in [14] by using a gain and offset correction loop, in conjunction with the calibration loops, to maximize the symmetry between the two channels.

A completely different technique, employed in [11], makes use of Lagrange interpolation to estimate the value of the input signal and cancel its effect on the error estimation process. This is done by calibrating the pipeline once every $M + 1$ samples ($M = 19$ in that paper) and using the previous and the successive M samples for the estimation, by using an FIR filter to implement the interpolation. Despite the fact that most samples are not used for calibration, a faster convergence is achieved because interpolation cancels most of the interference due to the input signal. However, this technique can be successfully used only if interpolation is accurate, and this imposes more stringent conditions on the input signal than simply to be band-limited. Moreover, the technique requires additional digital hardware, including a FIR filter for the interpolation.

In [14] a signal dependent PRBS is employed to avoid over-range after the PRBS insertion and to improve the number of samples that can be used in the estimation procedure, since in most techniques calibration is possible only if the input signal sample is contained in certain intervals, so that many samples may be useless for the parameter estimation. However, this technique requires additional capacitors, with an increase in the number of error parameters to be estimated.

The main limitation of the proposed technique is that the product of two different colored PRBS will have power concentrated around DC, so that it will be difficult to filter out. While the input-dependent power is mainly concentrated outside the bandwidth of the calibration filter, the terms due to the products among different colored PRBS will be mainly concentrated in that frequency region. However, these products are proportional to the error estimate, so that they are in general much smaller than the term given by the input signal. While it is possible to obtain a 25–30 dB of reduction in the power of the input-dependent term, the mixed terms will be amplified by a similar amount. Figure 15 shows the spectrum of the product of two noise sequences, in case of white and colored spectra.

6. CONCLUSION

A modification to the background calibration procedure by correlation has been presented, that allows faster convergence with lower estimation errors. The technique can be applied when the input signal to the ADC does not contain

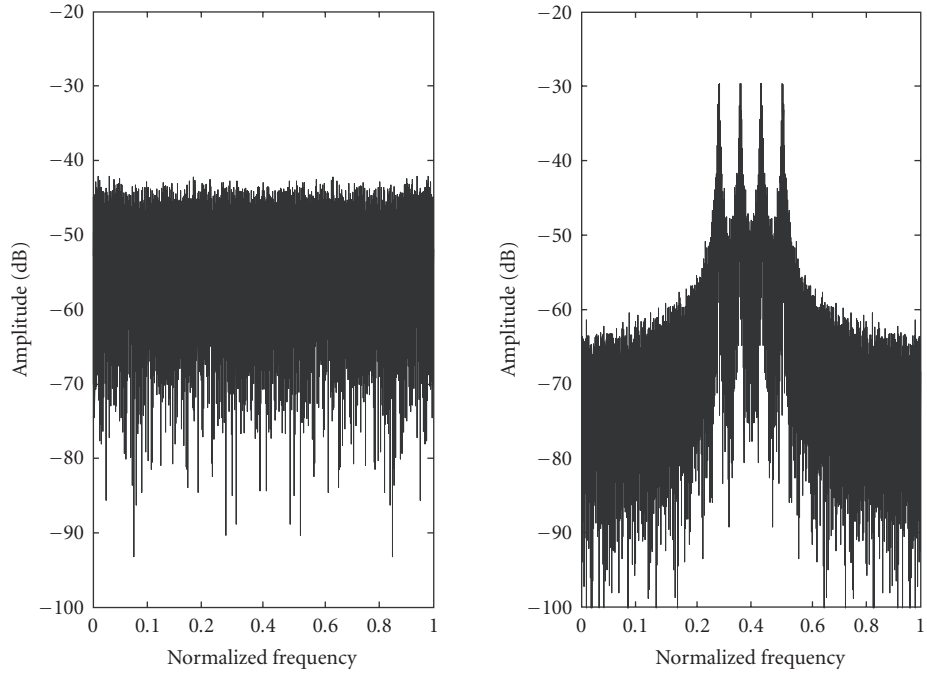

Figure 13: Power density spectrum of $P_N V_i$: (a) white noise; (b) colored sequence.

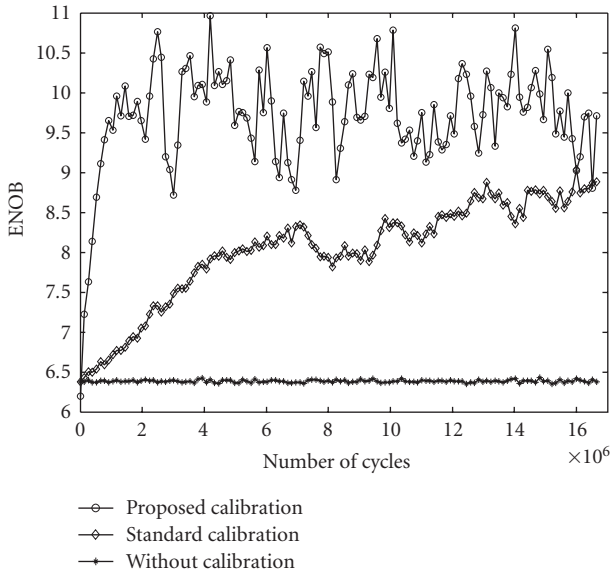

Figure 14: Transient evolution of the ENOB during calibration.

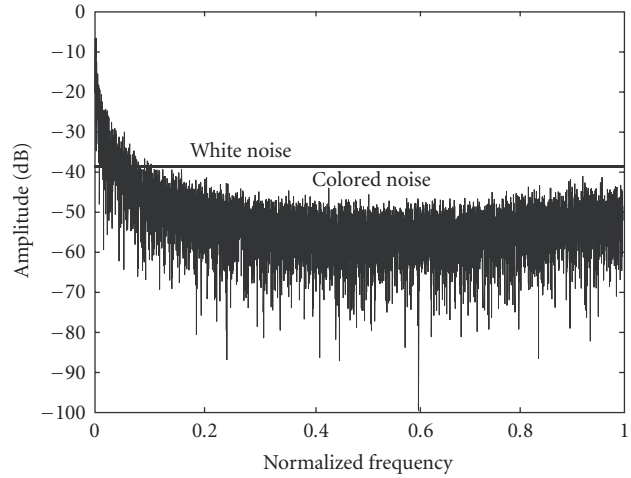

Figure 15: Spectrum of the product of two random sequences.

information around dc or $f_S/2$, and requires the use of a colored random sequence instead of a white sequence. This improves the SCNR of the estimation of the calibration parameter, and allows more flexibility in the choice of the lowpass filter used for the estimation. A practical circuit to generate a random sequence with the desired spectral properties has been proposed, that provides a more efficient implementation than lowpass filter in a PRBS signal. Monte Carlo simulations in Matlab show the advantages of the proposed method both in terms of estimation error and in improvement of the SFDR.

The proposed calibration technique is very simple to implement, requiring only additional combinational logic with respect to the technique by Moon and Li to generate the colored random sequence, and does not impose limitations on the input signals to the converter, a part from a little bandwidth penalty on the analog bandwidth.

REFERENCES

[1] J. Sevenhans and Z.-Y. Chang, "A/D and D/A conversion for telecommunication," *IEEE Circuits and Devices Magazine*, vol. 14, no. 1, pp. 32–42, 1998.

[2] Y.-M. Lin, B. Kim, and P. R. Gray, "A 13-b 2.5-MHz self-calibrated pipelined A/D converter in 3-μm CMOS," *IEEE Journal of Solid-State Circuits*, vol. 26, no. 4, pp. 628–636, 1991.

[3] H.-S. Lee, "A 12-b 600 ks/s digitally self-calibrated pipelined algorithmic ADC," *IEEE Journal of Solid-State Circuits*, vol. 29, no. 4, pp. 509–515, 1994.

[4] S.-U. Kwak, B.-S. Song, and K. Bacrania, "A 15-b, 5-Msample/s low-spurious CMOS ADC," *IEEE Journal of Solid-State Circuits*, vol. 32, no. 12, pp. 1866–1875, 1997.

[5] O. E. Erdoğan, P. J. Hurst, and S. H. Lewis, "A 12-b digital-background-calibrated algorithmic ADC with -90-dB THD," *IEEE Journal of Solid-State Circuits*, vol. 34, no. 12, pp. 1812–1820, 1999.

[6] J. M. Ingino and B. A. Wooley, "A continuously calibrated 12-b, 10-MS/s, 3.3-V A/D converter," *IEEE Journal of Solid-State Circuits*, vol. 33, no. 12, pp. 1920–1931, 1998.

[7] I. Galton, "Digital cancellation of D/A converter noise in pipelined A/D converters," *IEEE Transactions on Circuits and Systems II*, vol. 47, no. 3, pp. 185–196, 2000.

[8] J. Ming and S. H. Lewis, "An 8-bit 80-Msample/s pipelined analog-to-digital converter with background calibration," *IEEE Journal of Solid-State Circuits*, vol. 36, no. 10, pp. 1489–1497, 2001.

[9] J. Li and U.-K. Moon, "Background calibration techniques for multistage pipelined ADCs with digital redundancy," *IEEE Transactions on Circuits and Systems II*, vol. 50, no. 9, pp. 531–538, 2003.

[10] J. McNeill, M. C. W. Coln, and B. J. Larivee, ""Split ADC" architecture for deterministic digital background calibration of a 16-bit 1-MS/s ADC," *IEEE Journal of Solid-State Circuits*, vol. 40, no. 12, pp. 2437–2445, 2005.

[11] R. G. Massolini, G. Cesura, and R. Castello, "A fully digital fast convergence algorithm for nonlinearity correction in multistage ADC," *IEEE Transactions on Circuits and Systems II*, vol. 53, no. 5, pp. 389–393, 2006.

[12] S. H. Lewis and P. R. Gray, " A pipelined 5-Msample/s 9-bit analog-to-digital converter," *IEEE Journal of Solid-State Circuits*, vol. 22, no. 6, pp. 954–961, 1987.

[13] J. Rajski, N. Tamarapalli, and J. Tyszer, "Automated synthesis of phase shifters for built-in self-test applications," *IEEE Transactions on Computer-Aided Design of Integrated Circuits and Systems*, vol. 19, no. 10, pp. 1175–1188, 2000.

[14] J.-L. Fan, C.-Y. Wang, and J.-T. Wu, "A robust and fast digital background calibration technique for pipelined ADCs," *IEEE Transactions on Circuits and Systems I*, vol. 54, no. 6, pp. 1213–1223, 2007.